Advances in Process Analysis and Development in the Forest Products Industry

Kermit L. Holman and
W. James Frederick, Jr., editors

Advances in Process Analysis and Development in the Forest Products Industry

Kermit L. Holman and
W. James Frederick, Jr., editors

Arund Atreya
William A. Barkley
William R. Brown
W.C. Ricky Chan
David T. Clay
G.H. Covey
B.A. Crowell
L.L. Edwards
W.J. Frederick, Jr.
Edward J. Fritz
M.P. Godsay
R.E. Harrison
H.K. James
Frederick A. Kamke
Ferhan Kayihan
Barbara B. Krieger
Kenneth K. Kurple
Marina Neyman
E.M. Pearce
Kenneth W. Ragland
Scott Rumage
Robert W. Sackallares
N. Shiang
Edwin E. Smith

AIChE Symposium Series

Number 246 1985 Volume 81

Published by

American Institute of Chemical Engineers

345 East 47 Street New York, New York 10017

AIChE shall not be responsible for statements or opinions advanced in papers or printed in its publications.

Library of Congress Cataloging in Publication Data
Main entry under title:

Advances in process analysis and development in the forest products industries.

(AIChE symposium series ; no. 246, v. 81)

Papers in this volume were presented at symposia at the 1984 Annual Meeting of the American Institute of Chemical Engineers in San Francisco on November 25-30"—Foreword.

Organized by the Forest Products Division.

Contents: A study of the sensitivity of energy recovery to design and operating parameters in a DARS plant / W.J. Frederick, Jr., G.H. Covey and R.E. Harrison — Physico-chemical properties of cellulose oxidized by ozone / M.P. Godsay and E.M. Pearce — Antixolvent extraction of lignin / Marina Neyman ... [et al.] — [etc.]

1. Forest products industry—Congresses. I. Holman, Kermit L., 1935- . II. Frederick W. James (William James), 1945- . III. American Institute of Chemical Engineers. Meeting (76th : 1984 : San Francisco, Calif.) IV. American Institute of Chemical Engineers. Forest Products Division. V. AIChE symposium series ; no. 246.

TS802.A37 1985 674 85-30701

ISBN 0-8169-0354-9

Printed in the United States of America by
Twin Production & Design

FOREWORD

The papers in this volume were presented at symposia at the 1984 Annual Meeting of the American Institute of Chemical Engineers in San Francisco on November 25-30.

The papers in this volume present information useful to industrial practitioners in our field and yet serve academic staff who wish to gain insight into problems and solutions in the forest products industries. Those papers which are oriented toward applications sometimes are not available in printed form and yet are of major interest to chemical engineers in industry.

The topics presented include recent advances in delignification, evaluation of thermal properties of kraft black liquor, combustion and thermal degradation phenomena, and modeling, simulation, and control.

We wish to thank the authors of the papers contained herein for their contribution. Special thanks are extended to A.J. Chase, L.L. Edwards, A.L. Fricke, J.M. Genco, and F. Kayihan, who organized the sessions for the Forest Products Division. In addition we wish to acknowledge the timely assistance of the reviewers of the manuscripts.

Kermit L. Holman
Weyerhaeuser Paper Company
Tacoma, Washington 98477

W. James Frederick, Jr.
Department of Chemical Engineering
Oregon State University
Corvallis, Oregon 97331

CONTENTS

A STUDY OF THE SENSITIVITY OF ENERGY RECOVERY TO DESIGN AND OPERATING PARAMETERS IN A DARS PLANT

W.J. Frederick, Jr. ■ Dept. of Chemical Engineering, Oregon State University, Corvallis, Oregon 97331
G.H. Covey ■ Australian Paper Manufacturers Ltd., Morwell, Victoria, 8340 Australia
R.E. Harrison ■ Weyerhaeuser Technology Center, Tacoma, Washington 98477

A study was made to determine the sensitivity of energy recovery with the Direct Alkali Recovery System (DARS) to process parameters. The study was based on a steady-state model of the DARS process and data obtained from extensive pilot plant studies. Results indicate that the variables which most influence thermal efficiency in a DARS plant are the Na/Fe ratio, the quantity of fine Fe_2O_3 particles which must be removed from the white liquor after filtration, and the water content of the Fe_2O_3 streams returned to the reactor.

INTRODUCTION

The Direct Alkali Recovery System (DARS) is a process for regenerating NaOH from spent liquors from alkaline, non-sulfur pulping processes. The DARS process has been studied in detail and piloted by the Australian Paper Manufacturers, Ltd. (APM) (1,2,3). DARS is of interest as it can be employed with soda AQ pulping to give a simpler, cheaper and more odor-free process than conventional kraft pulping.

The objective of this study was to estimate the thermal efficiency of a DARS plant and its sensitivity to process parameters. A mass and energy balance model was developed which is used to calculate mass and energy flows based on key parameters specified for the process. Many of these parameters cannot be predicted but must be determined by measurement from laboratory or pilot plant experiments. The experimental data used in this model were obtained from laboratory and pilot experiments run by APM. They were used in the DARS mass and energy balance model to calculate a base case mass and energy balance and to determine the sensitivity of mass and energy flows to each of the key parameters.

This paper describes the mass and energy balance model and the assumptions and data used to develop it, and presents results of the sensitivity study. The data obtained from APM is proprietary and is not presented in this paper. Other data used in the model are available in the open literature and are included in this paper along with literature citations. The values and uncertainty of the key parameters for the mass and energy balance model are also discussed as are results of an analysis of the sensitivity of mass and energy flows to the key parameters.

DARS Mass and Energy Balance Model

Figure 1 shows the process flowsheet for a DARS plant. The process consists of the following unit operations.

1. A fluidized bed reactor in which spent pulping liquor is burned with iron oxide to form sodium ferrite ($Na_2O \cdot Fe_2O_3$). The fluidized bed block in Figure 1 also encompasses a boiler for steam generation and dust recovery and recycle equipment.

2. A leacher and filter in which sodium ferrite is hydrolyzed to form NaOH and the NaOH is leached from the solid phase. Most of the residual solid phase, which consists mainly of Fe_2O_3, is separated from the NaOH solution (white liquor) and is recycled to the fluidized bed reactor.

3. A clarification stage in which finely divided solid particles are removed from the white liquor.

4. A mix tank, in which spent pulping liquor and the recycled slurry from the clarification stage are mixed.

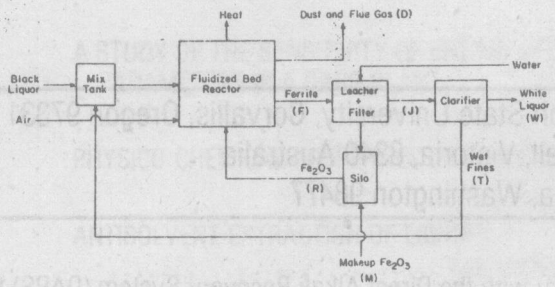

Figure 1.

The DARS process was modeled as a steady state process by a series of algebraic equations which describe the flows of mass and energy through the process. The model consists of mass and energy balances around each of the major operations in the process, the mix point for Fe_2O_3 makeup, and overall balances.

Overall mass balance

Sodium enters the DARS plant as black liquor and leaves as white liquor or as dust. Sodium makeup to the pulp mill is assumed to be added outside of the DARS plant boundary. The overall sodium mass balance for the DARS process is: $B[Na]_B = 0.742\ WC_W + D[Na]_D$ (1)

The white liquor flow rate from the DARS plant is calculated from equation 1 once the black liquor flow rate and composition and the dust loss from the fluidized bed stack and its composition are specified.

Ferrite Leacher Balance

The following parameters must be specified to describe the leaching system:

Ferrite Na/Fe mole ratio ($(Na/Fe)_{Bed}$)

White liquor concentration (C_W)

Suspended solids mass fraction in white liquor before clarification (Y_J)

Recycled Fe_2O_3 total (dissolved + suspended) solids mass fraction (X_R)

Na/Fe mole ratio in recycled Fe_2O_3 ($(Na/Fe)_R$)

The causticity (η_{caust}) for the entire system (except black liquor) was assumed to be constant. The term causticity is used to refer to the ratio of NaOH to NaOH plus Na_2CO_3 in solution or $Na_2O \cdot Fe_2O_3$ to $Na_2O \cdot Fe_2O_3$ plus Na_2CO_3 in the solid phase, with all sodium compounds expressed on a Na_2O basis. Experiments have shown that causticity is almost independent of process parameters over the range of interest. A typical causticity of 94% has been used for this study except where noted otherwise.

The overall balances for the leaching system for Na_2O and Fe_2O_3 are

$$F[Na_2O]_F = C_W W + J(1-Y_J)C_W + RX_R[Na_2O]_R \quad (2)$$

and

$$F[Fe_2O_3]_F = J\,Y_J + RX_R[Fe_2O_3]R \quad (3)$$

where, from stoichiometric considerations, (see appendix),

$$[Na_2O]_F = \frac{.3882\ (Na/Fe)_F}{1 + .3882(na/Fe)_F(1.710-0.71\eta_{caust})} \quad (4)$$

$$[Na_2O]_R = \frac{.3882\ (Na/Fe)_R}{1 + .3882(Na/Fe)_R(1.710-.4194\eta_{caust})} \quad (5)$$

$$[Fe_2O_3]_F = \frac{1}{1 + .3882(Na/Fe)_F(1.710-0.710\eta_{caust})} \quad (6)$$

and

$$[Fe_2O_3]_F = \frac{1}{1 + .3882(Na/Fe)_R(1.710-.4194\eta_{caust})} \quad (7)$$

With the Na_2O and Fe_2O_3 mass fractions specified, equations 2 and 3 contain three unknowns: F, J and R. The third equation needed to solve for them is determined from the specified split of Fe_2O_3 recycled directly to the fluidized bed and the fines leaving the leacher with the white liquor:

$$J(Y_J - Y_W(1-Y_J)C_W) = WC_W\,Y_W \quad (8)$$

Equations 2, 3 and 8 are solved simultaneously for F, J and R.

Fluidized Bed and Dust Collection System

A fraction of the inorganics entering the fluidized bed leave the bed as dust entrained

in the flue gas. The Na and Fe flows in and out of the fluidized bed/dust collection system are all specified from equations 1, 2, 3 and 4. The recycled dust loses a small amount of heat but has a minimal impact on the overall thermal efficiency of a DARS plant. The heat loss depends more on dust handling equipment design than on process operation. Therefore it was not treated separately but was assumed to be part of the "unaccounted losses" in the heat balances.

Chemical Makeup Requirements

The chemical makeup requirements for the DARS plant (i.e. excluding makeup for pulp mill chemical losses) are calcualted from mass balances and are based on the dust loss from the fluidized bed stack and its composition:

$$\text{Na makeup} = D[\text{Na}]_D\ (2.304 - .565\ \text{caust}) \quad (10)$$

$$\text{Fe makeup} = \frac{3.472\ D\ [\text{Na}]_D}{(\text{Na/Fe})_D} \quad (11)$$

Energy Balances

Energy balance calculations were made around each process block (Figure 1) and around the entire DARS process. The DARS reactor balance was made assuming that the difference between the sums of the heat inputs and outputs was recoverable as useful energy (steam, etc). Two considerations in the DARS reactor heat balance require further comment. First, the heating value and elemental compostion of the black liquor solids were assumed to be a function only of the causticity of the white liquor produced by the DARS plant. This assumption was made because the inorganic/organic ratio in the black liquor solids varies inversely with the causticity and because of our earlier assumption that other pulp mill parameters (yield, kappa, chemical charge, etc.) do not change. Table 1 shows how the heating value and elemental composition of black liquor varies with causticity. The data are from calculations made using heating value and composition data from a North American pulp mill to estimate the composition and heating value of dissolved wood organics. The flow and composition of the dissolved wood organics per ton of pulp are the same for the three causticities in Table 1.

The second consideration in the DARS reactor heat balance requiring comment is the heat of reaction to form sodium ferrite ($Na_2O{\cdot}Fe_2O_3$) from Fe_2O sodium in the black liquor, and oxygen. This can be considered as a sequential reaction series in which

$$\text{BLS (Na, C)} + O_2 \rightarrow Na_2CO_3 \quad (12)$$

$$Na_2CO_3 + Fe_2O_3 \rightarrow Na_2O{\cdot}Fe_2O_3 + CO_2 \quad (13)$$

Reaction 13 accounts for the formation of sodium ferrite from Na_2CO_3 produced by combustion of black liquor. Its heat of formation, estimated from heat of formation data (4), is +233.9kJ/mole sodium ferrite. It is independent of the chemical form of Na in the black liquor since that is accounted for in the heat of combustion of black liquor.

Recycled NaOH also reacts with Fe_2O_3 in the DARS reactor. The net impact of recycled NaOH on the energy balance for the DARS plant is zero based on the constant causticity assumption. However, the net (zero) heat release is the sum of two parts: an endothermic reaction given by equation 14

$$2\ NaOH + Fe_2O_3 \rightarrow Na_2O_3 + H_2O \quad (14)$$

which occurs in the reactor and the exothermic reverse reaction which occurs in the leacher. Although the net heat effect is zero, the cycling of recycled NaOH betweed NaOH and $Na_2O{\cdot}Fe_2O_3$ affects the individual heat balances for the DARS reactor and the leacher. The heat of reaction for equation 14, estimated from heat of formation data (4,5), is +67.36 kJ/mole sodium ferrite. No heat of reaction was included for the Na_2CO_3 recycled with Fe_2O_3 because of the assumption of constant causticity throughout the DARS plant.

Table 1. Black Liquor Solids Composition and Heating Value Versus Causticity.

Causticity, %	85.8	94.0	94.4
Black Liquor Solids Composition, mass fraction			
Na	.2074	.1976	.1971
C	.3747	.3861	.3866
H	.0421	.0439	.0440
O	.3758	.3724	.3722
Black liquor solids heating value, kJ/kg	13,143	13,714	13,741

In the leaching system heat balance, sodium ferrite was assumed to be converted completely to NaOH and Fe_2O_3. The heat of the hydrolysis reaction (including dilution) is approximately -106.6 kJ/mole sodium ferrite; the exact value is a weak function of concentration.

Energy balances for the other DARS process blocks are enthalpy balances for blocks in which no chemical reactions occur. These blocks include the sodium ferrite cooler/air pre-heater (direct contact exchanger) for the DARS reactor, the mix tank, and the dust separator. Table 2 contains the heat capacity relationships for the various DARS process streams and components that were used in the model.

Table 2. Heat Capacities Used in the DARS Process Energy Balances

Stream	Cp, kJ/kg °C
Black liquor	8.71 2 + XBL
White liquor	4.187 - 3.30 C_w
Sodium ferrite (6)	0.946 (25 - 500°C) 1.06 (1100°C)
Recycled Fe_2O_3 and Fe_2O_3 fines mud	4.187 - 3.24X
Dust	1.05
Air	1.01
Dry flue gas	1.00
Water vapor	1.88

Sensitivity of Recoverable Energy to DARS Plant Design and Operation

The objective of the sensitivity study was to determine how net energy recovered from a DARS plant varied with design and operating parameters. In the study, the pulp mill associated with DARS plant was assumed to operate at constant pulp production and yield with an unchanging wood supply. On this basis, changes in DARS plant energy recovery are attributable to changes in DARS plant operation only. Table 3 contains the data used in the base case calculations and the range of variables considered in the sensitivity study. Table 4 shows the other input variables that were held constant during the study.

Base case

The base case for the sensitivity study was based on a white liquor concentration of 300 g NaOH/liter at 94% causticity (0.193kg Na_2O/kg white liquor). Table 3 contains the other DARS plant boundary conditions assumed for the base case. Other process parameters were taken from the proprietary APM data and are not presented here.

Table 3. DARS Process Boundary Conditions For Sensitivity Study

Input Parameter	Value
Black liquor solids mass fraction to mix tank	.65
Black liquor solids higher heating value	13,714 $\frac{kJ}{kg}$
Black liquor solids composition (mass fraction)	Na .1976 C .3861 H .0439 O .3724
Temperature of black liquor to mix tank	95°
Dust lost to atmosphere with flue gas	18 kg/kg BLS
Oxygen mole fraction in dry flue gas	.03
Unaccounted heat loss/heat input ratio for reactor	.025
Air temperature to DARS reactor	25°C

Table 4. Base Case Stream Composition (Basis: 1 Kg Black Liquor Solids)

Stream	Mass Flow kg/kg	Heat Flow 10^3kJ/kg	Temp °C
Black liquor to mix tank	1.581	.350	95
Wet fines to mix tank	0.508	.116	144
Black liquor from mix tank	1.047	.466	104
Ferrite to leacher	2.288	.172	100
Water to leacher	1.471	.185	55
White liquor	1.396	.593	144
Recycled Fe_2O_3	1.855	.071	55
Dry flue gas	5.713	.577	125
Water in flue gas	1.208	3.216	125
Dust lost to atmosphere	.0012	.0001	125
Air to fluid bed	5.386	0	25
Fe_2O_3 makeup	.0008	0	25

Table 4 shows the mass balance results for the base case. The high white liquor and wet fines temperatures (144°C) result from the heat released in the hydrolysis reaction. In practice this heat would be removed by evaporation or by cooling the white liquor indirectly.

The energy balance for the base case is summarized in Table 5. The fluidized bed heat balance is divided into heat inputs, heat losses and high pressure steam generated. The steam generation rate for the base case is 9.264×10^3 kJ/kg black liquor solids, corresponding to a thermal efficiency (steam generated/total heat input) of 65.1%. Table 5 also shows the heat released by hydrolysis of $Na_2O \cdot Fe_2O_3$ during leaching for the base case.

Table 5. Base Case Heat Balance Summary

	10^3 kJ/kg	% Total Input
I. Fluidized Bed		
Inputs:		
Black Liquor HHV	13.714	96.43
Black Liquor Sensible Heat (from mix tank)	0.436	3.07
Fe_2O_3 Sensible Heat	0.071	0.50
Air Sensible Heat	0.000	0.00
Total Input:	14.221	100.00
Losses:		
Dry Flue Gas	0.577	4.06
Water in Flue Gas	3.116	21.95
Ferrite Sensible Heat	0.172	1.21
Heat to form Sodium Ferrite	0.736	5.18
Unaccounted Losses	0.356	2.50
Total losses:	4.957	34.89
Heat to Steam	9.264	
Thermal Efficiency		65.10
II. Leacher		
Hydrolysis of $Na_2O \cdot Fe_2O_3$	0.424	2.98

The energy balance for the base case is summarized in Table 5. The fluidized bed heat balance is divided into heat inputs, heat losses and high pressure steam generated. The steam generation rate for the base case is 9.264×10^3 kJ/kg black liquor solids, corresponding to a thermal efficiency (steam generated/total heat input) of 65.1%. Table 5 also shows the heat released by hydrolysis of $Na_2O \cdot Fe_2O_3$ during leaching for the base case.

Maximum recoverable energy

The first case examined in the sensitivity study was the maximum recoverable energy from the DARS process. The maximum recoverable energy was taken to be the steam generated when

1. All Fe_2O_3 is recycled free of water and sodium salts.
2. ferrite cooled to 100°C,
3. no dust leaves the reactor.

This situation represents an ideal upper limit for steam generation based on the assumption of perfect separation of suspended Fe_2O_3 from white liquor. Although it is not obtainable in practice it provides a convenient reference for comparing more realistic cases. The only losses included are heat to form sodium ferrite, ferrite and flue gas sensible heat, heat to evaporate water, and unaccounted losses.

The results are presented in Table 6 along with the base case results. The heat losses are separated into two categories: those controlled by DARS parameters and those determined by factors external to the DARS reactor. The DARS parameters account for 11.1% of the heat input as losses in the base case. This is reduced to 6.0% in the maximum recoverable energy case. The losses determined external to the reactor are essentially constant (percentage increases because total heat input decreases). The steam generation rate increases by 6.4%, from 9.264×10^3 kJ/kg black liquor solids[1].

Table 6. Heat Balance for Base Case Versus Recoverable Energy Case[a].

	Base	Maximum Recoverable Energy
I. Total Heat Input, 10^3 kJ/kg	14.221	14.118
II. Controlled by DARS Parameters, % of Input		
Evaporation of Water		
From wet fines	2.14	0.00
From recycled Fe_2O_3	2.60	0.00
Heat to Form Ferrite	5.16	4.94
Ferrite Sensible Heat	1.20	1.07
Total	11.10	6.01
III. Controlled By Factors External to Reactor, % of Input		
Evaporation of Water		
Water in black liquor	9.50	9.57
Water formed by combustion	7.71	7.77
Dry Flue Gas	4.05	4.09
Unaccounted Losses	2.50	2.50
Total	23.76	23.93
IV. Combined Total Heat Losses, % of Input	34.86	29.94
Thermal Efficiency	65.14	70.06
V. Steam Generated by Reactor, 10^3 kJ/kg	9.264	9.892

[a]Basis: All Fe_2O_3 recycled free of water and sodium salts; ferrite leaves cooler at 100°C; no dust leaves the reactor.

[1]The energy flows in the sensitivity cases are expressed relative to the black liquor solids flow in the base case.

Summary of Sensitivity Study Cases

Changes in DARS parameters affect both mass and energy flows in the process. The sensitivity of DARS mass and energy flows to DARS parameters was determined by varying the parameters of interest one at a time in the DARS process model. The upper and lower limits for each variable were estimated from pilot plant data and from operating performance of similar equipment in similar applications. These limits indicate the maximum uncertainty in each of the DARS parameters.

Tables 7 and 8 contain the percent changes in the DARS parameters used in the sensitivity study (relative to the base case value) and the resulting percent changes in mass flow rate or high level energy recovery.

Table 7. Impact of DARS Parameter Changes on Total Mass Flow Rates. (Data as Percent Change in Mass Flow Rate).

Parameter	Na/Fe Mole Ratio In Reactor Product	White Liquor Concentration	Recycled Fe_2O_3 Suspended Solids Conc.	Suspended Fines/Na_2O Ratio in White Liquor Before Clarification	Suspended Fines Concentration To Reactor
% change	- 52	- 33	- 11	+ 200	- 33
Impact On: Wet Fines to Mix Tank				+ 323	+ 83
Reactor Product to Leacher	+ 104			+ 39	+ 22
Black Liquor from Mix Tank				- 83	+ 3
Water to Leacher	+ 18	+ 36	+ 16	+ 36	+ 2
White Liquor		+ 18			
Recycled Fe_2O_3 from Leacher	+142		+ 13		+ 4
Water in Flue Gas	+ 13		+ 19	+ 39	+ 26

Mass balance impacts

Table 7 shows the change in total mass flows for those streams increasing by more than 10% when a DARS parameter is varied to its upper or lower uncertainty limit as estimated from the pilot plant data. Results are shown only for the direction of change which increases the size of process equipment.

The parameters which affect the most process streams are Na/Fe mole ratio in the reactor product, wet fines suspended solids/white liquor Na_2O ratio, and wet fines suspended solids content. Changes in wet fines mass flow rate and solids concentration directly affect the size of the fines separation and handling equipment, the reactor feed pump size, the size of the induced draft fan for the reactor, the water flow rate to the leacher, and water pump size. Changes in reactor product Na/Fe mole ratio affect leacher size, reactor product and recycled Fe_2O_3 handling equipment, induced draft fan size, and water to the leacher.

Energy balance impacts

Table 8 shows the impact of DARS parameters on high level energy recovery for a DARS plant. The parameters are varied to the limits of uncertainty determined from pilot plant data. Results for both uncertainty limits (minimum, maximum parameter values) are included.

Table 8. Impact of DARS Parameter Changes on High Level Energy Recovery

Parameter	Base Case	% Change	Change in High Level Energy Recovery, %
Na/Fe Mole Ratio in Reactor Product	.418	- 52 + 91	- 7.65 + 2.04
Suspended Fines/Na_2O Ratio in White Liquor Before Clarification	1.0	- 90 +200	+ 3.44 -12.51
Suspended Fines Concentration to Reactor	.60	- 33 + 33	- 8.56 + 3.22
Recycled Fe_2O_3 Mass Fraction	.90	- 11 + 5.5	- 6.3 + 2.66
Na/Fe Mole Ratio in Recycled Fe_2O_3	.02	+150 - 75	+ 0.86 + 0.38
White Liquor NaOH Concentration, g/l	300	- 33 + 33	- .04 + .04
Maximum Energy Recovery Case	--	--	+ 7.08

The variables with the greatest impact on energy recovery are Na/Fe mole ratio in the reactor product, wet fines suspended solid/white liquor Na_2O ratio, wet fines suspended solids content, and recycled Fe_2O_3 solids content. In most cases the relationships between DARS parameters and energy recovery are not linear, and changing a parameter in the direction of lower energy recovery has a greater impact than a change in that parameter of the same magnitude but in the opposite direction.

Conclusions

The thermal efficiency for a DARS plant, based on the parameters used in this study, is about 65%. The thermal efficiency varies with pulping process conditions as well as with DARS plant design and operating parameters.

The thermal efficiency is sensitive to process design parameters. The variables with the greatest impact are the Na/Fe mole ratio in the reactor product, the suspended fines/Na_2O ratio in the white liquor before

clarification, and the water content of the wet fines and the recycled Fe_2O_3. Designs which increase the Na/Fe mole ratio in the reactor product and decrease the other three parameters will be more efficient.

The maximum thermal efficiency which can be attained in the DARS process is about five percent greater than the base case thermal efficiency, and corresponds to a 6.4% increase in steam generated. This result is based on the assumption that DARS plant parameters are optimized but that conditions external to the DARS plant (spent pulping liquor composition, etc.) are not changed.

Equipment capacity requirements for the DARS plant are sensitive to the Na/Fe mole ratio in the sodium ferrite, the white liquor concentration, the suspended fines/Na_2O ratio in the white liquor before clarification, and the water content of the wet fines and the recycled Fe_2O_3. The size of the fluidized bed reactor and the leacher are influenced most by the Na/Fe mole ratio in the sodium ferrite.

Acknowledgements

The authors would like to thank Australian Paper Manufacturers Ltd. and Weyerhaeuser Company for permission to publish this information.

LITERATURE CITED

1. Covey, G. H., "Development of the Direct Alkali Recovery System and Potential Applications," Proceedings of the International Conference on Recovery of Pulping Chemicals, Vancouver, B.C., September, 1981, p. 181-184.

2. Covey, G. H., Keogh, A. J. and Nguyen, K. L., "An Introduction to the Direct Alkali Recovery Process," Presented at the 36th General Appita Conference, March 29 to April 2, 1982, Launceston, Tasmania.

3. Covey, G. H., "DARS - The Direct Alkali Recovery System". Notes from the Pacific Section TAPPI 37th Annual Seminar, Corvallis, OR (September 13-14, 1984).

4. Perry, J. H., Chemical Engineers' Handbook 4th Ed., McGraw-Hill Book Company, New York (1963) p. 3-134.

5. Mellor, J. W., Inorganic and Theoretical Chemistry, Vol. XIII. Longman, Green and Company, New York (1934) p. 907.

6. Barin, I. and Knacke, O. Thermochemical Properties of Inorganic Substances, Springer-Verlag, Berlin (1973) p. 551.

Table of Symbols

Symbol	Definition
B	mass flow rate of black liquor solids
C	mass ratio of total sodium salts (as Na_2O) to white liquor
C_p	heat capacity
D	mass flow rate of dust lost to atmosphere
F	mass flow rate of reactor product (mainly sodium ferrite)
$[Fe_2O_3]$	iron oxide mass fraction, dry solids basis
ΔH_v	heat of vaporization of water
J	mass flow rate of unclarified white liquor from leacher
Na/Fe	sodium/iron mole ratio
[Na]	sodium mass fraction, dry solids basis
$[Na_2CO_3]$	sodium carbonate mass fraction, dry solids basis
$[Na_2O]$	sodium oxide mass fraction, dry solids basis
R	mass flow rate of leached solids (mainly Fe_2O_3) recycled from leacher to DARS reactor
W	mass flow rate of white liquor
X	total solids mass fraction
Y	suspended solids mass fraction
η_{caust}	fractional conversion of Na_2O_3 to $Na_2O \cdot Fe_2O_3$

Subscript	Definition
B	black liquor solids
D	dust lost to atmosphere
F	DARS reactor underflow (mainly sodium ferrite)
J	from leacher, before clarification
R	leached solids (mainly Fe_2O_3) recycl from leacher to DARS reactor
W	white liquor

APPENDIX

The concentrations of Na_2O and Fe_2O_3 in the DARS process streams are determined as follows. We assumed that the fluidized bed product (ferrite) contained only $Na_2O \cdot Fe_2O_3$, Na_2CO_3 and Fe_2O_3. The following equations are based on the mole ratio of Na/Fe in the stream.

The ratio of mass of Na_2O/mole Fe in the ferrite stream is

$$\text{mass of } Na_2O/\text{mole Fe} = 31\,(Na/Fe)_F \quad \text{(A-1)}$$

where the Na_2O in this equation is based on the total sodium (from both $Na_2O \cdot Fe_2O_3$ and Na_2CO_3).

The total mass of suspended solids/mole Fe is the sum of the masses of Na_2O (from $Na_2O \cdot Fe_2O_3$), Na_2CO_3 and Fe_2O_3 (from $Na_2O \cdot Fe_2O_3$ and the uncombined Fe_2O_3. It depends on the fractional conversion of Na_2CO_3 to $Na_2O \cdot Fe_2O_3$:

$$\text{Total mass/mole Fe} = 31(Na/Fe)_F\, c_{aust} + 53(Na/Fe)_F(1 - c_{aust}) + 79.85(Fe/Fe)_F \quad \text{(A-2)}$$

Where the ratio (Fe/Fe) is 1.0. dividing equation A-1 by A-2 and rearranging gives

$$[Na_2O]_F = \frac{0.3882(Na/Fe)_F}{1 + 0.3882(Na/Fe)_F(1.710 - .710\, c_{aust})} \quad \text{(A-3)}$$

Where $[Na_2O]$ is the mass fraction of Na_2O in the stream based on total (dissolved plus suspended) solids.

Equation A-3 is the same as equation 4 in the text. The corresponding relationship for Fe_2O_3 (equation 6) is derived the same way. The mass of Fe_2O_3/mole Fe is half the molecular weight of iron oxide (79.85). Dividing it by equation A-2 and rearranging gives equation 6.

Equation 5 and 7 which are for the recycled iron oxide stream are developed the same way. The total mass of solids in this case consists of NaOH, Na_2CO_3 and Fe_2O_3 since all the $Na_2O \cdot Fe_2O_3$ is assumed to be hydrolyzed. The total mass/mole Fe is:

$$\text{Total Mass/mole Fe} = 40(Na/Fe)_R\, c_{aust} + 53(Na/Fe)_R(1 - c_{aust}) + 79.85(Fe/Fe)_R \quad \text{(A-4)}$$

Equation 5 is developed by dividing equation A-1 by A-4, while equation 7 results from dividing half the molecular weight of Fe_2O_3 by equation A-4.

PHYSICOCHEMICAL PROPERTIES OF CELLULOSE OXIDIZED BY OZONE

M.P. Godsay ■ International Paper Company, P.O. Box 797, Tuxedo Park, NY 10987
E.M. Pearce ■ Polymer Research Institute, Polytechnic Institute of New York
333 Jay Street, Brooklyn, NY 11201

The objective of this investigation was to elucidate the mechanisms of cellulose-ozone reactions and determine the effect of different cellulose morphologies on the course of such a reaction. Ozonization was carried out in a stirred tank reactor which provided the capability of contacting large quantities of ozone to a specified volume of cellulose pulp slurry. The reactions were followed by means of time and % ozone consumption. The oxidized products were analyzed for degree of polymerization (DP) from which chain scissions were calculated. The oxidized products were also analyzed for functional groups.

Apparent reaction constants for ozone: cellulose reactions for cotton linters, chemical and paper pulps were calculated. The pseudo first order rate constants of the heterogenous reaction were found to be close to those of ozonization of methyl-β-glucopyranoside (MβG) carried out by Pan (*18*) under homogeneous conditions. Mode of attack of ozone on cellulose was thus found to be similar to the one observed by previous investigators on cellulose model compounds such as MβG. Results also show that cellulose morphology and the cellulose constituents such as xylans and mannans play an important role. Initial DP and cellulose accessibility also must be taken into consideration for the proper interpretation of ozone attack on cellulose. The anomalous DP and strength behavior of ozone oxidized cellulose was found to be due to the loss of DP during viscosity determination by the alkaline cupriethylenediamine (CED) procedure; and to the β-alkoxy elimination reactions due to the presence of ketonic functionality on oxidized cellulose.

INTRODUCTION

Reaction of cellulose polymer with oxidizing agents leads to chemical attack, and almost invariably to loss of physical properties such as tensile strength. Degradation of cellulosic fibers by oxidizing agents is one of the hazards of the bleaching processes. Minimizing the degradative attack on the cellulose while destroying the color is the major goal of any industrial bleaching process. Established textile or pulp bleaching processes are predominantly based on chlorine-containing oxidizing agents such as chlorine, hypochlorite and chlorine dioxide. Reactions of these compounds with lignocellulosic materials and their utilization in pulp bleaching have been thoroughly investigated (1, 2). Lewin (2) has recently extensively reviewed the literature on the bleaching of cellulosic and synthetic fibers. Nonchlorine bleaching agents such as oxygen and ozone are slowly gaining acceptance in the industry. This acceptance is mainly based on their potential in effluent-free bleaching processes. However, the bleached fibers, resulting from these processes, show lower degrees of polymerization (DP) as measured by standard viscosity measurement procedures (3). Dependence of end use properties such as strength, elongation, etc. of a polymer on the molecular weight or DP is well recognized. Many investigators (4-6) had noticed that the viscosity (DP) of ozone oxidized kraft pulps decreased rapidly with the increased oxidation. However, this decrease in DP was not accompanied by expected decrease in composite strength properties. Swenson (7) tried to explain this discrepancy by comparing absolute and intrinsic viscosities of oxidized pulps in cupriethylene diamine (CED) and alkaline ferric tartanate (FeTNa) and DP_N (number average) by osmometry and DP_W (weight average) by sedimentation. He found good correlation between DP_W and zero span (fiber) tensile strength and argued that the secondary bonds between cellulose and lignin are responsible for the observed behavior. Recent studies (8-9) on fully bleached pulps bleached with ozone show the same discrepancy between observed DP by viscometry and the composite's (paper's) tensile properties.

Although oxygen and ozone could be important future bleaching agents, the fundamental information regarding their behavior, their action on lignin, lignocellulose and cellulose is meager. The objective of the present Investigation is, therefore:

to investigate the fundamental reaction mechanism of the attack of ozone on cellulose polymer backbone; and

to attempt to explain the anomalous strength-DP behavior of ozone-bleached pulps.

Investigations discussed in this paper pertain mainly to ozone-cellulose reactions. Ozone-cellulose reactions in presence of lignin (pulp) are discussed elsewhere (10).

Doreé and Cunningham (11) and Doreé and Healey (12) investigated the action of ozone on cellulose, modified cellulose and cellulose derivatives. They noticed that cellulose-ozone reaction proceeded only in the presence of water, and the resulting products had high copper numbers indicating the presence of reducing groups. Thus the action of ozone resembled that of other oxidizing agents in acidic medium. Osawa (13) et al. observed the topochemical action of ozone on woodmeal and concluded that the leveling off degree of polymerization (D.P.) of native wood cellulose was much higher (400 D.P.) than the chemically treated celluloses (150-200 D.P.). Deslongchamps (14) et al. studied the action of ozone on a cellulose model, methyl-β-D-glucopyranoside (MβG), and found that the acetal function of the fully acetylated MβG reacts quantitatively with ozone in nonaqueous solvents; the corresponding α-anomer, however, was completely inert. They postulated an ozone insertion mechanism at C-1 as per Katai (15) et al. Pan (16) further elucidated this attack of ozone at the hydrogen at C-1 as a major process in the ozonization of MβG because of the presence of gluconic acid δ-lactone as a major product. Katai and Schuerch (15) found the carbonyl and carboxyl functions after the ozonization of MαG and methyl cellulose. The observed severe degradation of wood pulp by ozone was explained by their mechanism which involved an electrophilic attack of ozone on the carbohydrates to liberate the anomeric carbon via an ozone catalyzed hydrolysis of glucosidic bonds.

Oxidation of cellulose, in general, like hydrolysis, is a heterogeneous reaction. Attack occurs more rapidly in the amorphous regions of cellulose, followed by slower attack on the more ordered region. There are at least four places where an unhydroglucose unit will be subject to attack, as shown in Fig. 1.

Attack at 2-3 positions leads to keto groups or breaking of the ring, leading to aldehyde groups which may, in turn, be oxidized to carboxyl groups. These possibilities are shown in Fig. 1. With these numerous possibilities, analysis of the resulting oxycellulose with respect to the position of the specific group is difficult, especially since the chlorine-based oxidizing agents act in a non-specific manner. Some reagents such as periodic acid, nitrogen dioxide and lead tetraacetate are apparently more specific in their reactions. The properties of the oxycelluloses differ widely depending upon the nature of groups produced. Thus cellulose, treated with alkaline solutions of sodium hypobromite or hypochlorite, gives products with low reducing power (low copper number), but contains a large number of acid groups (as determined by absorption of basic dye, methylene blue). Reactions under acidic conditions lead to the opposite effect -- high copper numbers and low quantities of acid groups. Fiber degradation, sometimes, may not be apparent until the oxidized fiber comes in contact with alkali during hydrolysis of the cellulose chain resulting in a large DP loss.

Thus,

- the oxidative attack on cellulose by various oxidizing agents results in the formation of oxycellulose.
- these oxycelluloses differ in properties, depending upon the oxidizing agent. These agents may increase either carboxyl or aldehyde content, and in extreme cases will break the anhydroglucose ring or cellulose chain.
- most of the oxycelluloses are characterized by their extreme alkali sensitivity, resulting in a DP loss when treated with alkali.
- the characterization of the oxycelluloses is difficult due to the random nature of attack, the possibilities for hemiacetal and acetal formation, hydration and alkali sensitivity.

1) Ozonization of Various Celluloses

The samples of celluloses used in these experiments were as follows:

- Cotton Linters Samples
- Chemical Pulp (α-cellulose) - a prehydrolyzed cold caustic extracted hardwood kraft pulp sample without lignin and very little hemicelluloses
- Paper Pulps - a hardwood kraft paper pulp, bleached to remove only lignin

The composition of these samples is shown in Table 1. The composition shows that the cotton linters samples are 99.4% glucan. Chemical pulp consists of 97.4% glucan and 2.1% xylan, and paper pulps 77.6% glucan and 22.1% xylan.

These samples were ozonated in the ozone reactor described in Appendix 1. The results of Tables 2 through 4 show:

- cotton linters consumed more ozone than either chemical pulp or paper pulp within an equal time period. The plots of consumed ozone vs. time shown in Fig. 2 are linear and can be fitted by the following equation:

$$-d\,[O_3]/_{dt} = K_{O_3}\,[M]_0\,[O_3]_t \quad \ldots\ldots\ldots(1)$$

The relative rates of oxidation of various organic substances by ozone can be measured in a competing environment. The problems of ozone dissociation and radical interactions still remain. The criteria, as outlined by Hoigné (17) for pure direct ozone reactions were:

1) The kinetics remained first order in ozone and solute concentrations over the entire range measured.

2) Within the pH range employed small changes in pH did not affect the apparent rate constant.

We have used the pseudo first order kinetics in dealing with the reactions of ozone with lignin and cellulose. The above constraints, however, clearly do not apply for these reactions where pH change with reaction time and the nature of the oxidizable components change. Earlier workers realized these difficulties and restricted their efforts to model compounds studies only.

For the present purpose, however, the slopes of the plots of ozone consumed with time should represent the rate constants of oxidation and are expressed in m·moles of ozone per cellulose mole per min. The calculated rate constants for these three samples are:

Sample	K m·moles O_3 mole^{-} (cell) min^{-1}
Cotton	0.44
Paper Pulp	0.35
Chemical Pulp	0.275

The pseudo first order rate constants of various celluloses calculated in this study are strikingly close to those found for ozonization of MβG by Pan (18). These are compared in Table 5.

Thus it seems that the mode of attack of ozone on cellulose is quite similar to the one observed by previous investigators on cellulose model compounds such as MβG. However, the side reactions such as oxidation of the hydroxyl groups are completely suppressed in the model compounds. Besides, because of the low pH and low temperatures used by Pan (pH 5, 15°C), the free radical dissociations and ensuing reactions are minimized. In spite of these differences, the results of this investigation concur with previous observations.

It seems that the wood pulp is more resistant to oxidation than the very pure cotton cellulose. The reason(s) of this seeming resistance to degradation may be due to:

- morphological differences between wood and cotton celluloses. Cotton is morphologically Cellulose I, a structure very reactive to reagents. However, wood celluloses which have gone through a high temperature caustic digestion are morphologically closer to Cellulose II. Chemical pulp, after kraft cooking, has undergone an additional cold caustic treatment which will make it still less reactive. We have previously noticed in our laboratory that in the cellulose carbanilation, acetylation or carboxymethylation reactions, cotton is much more reactive than the wood pulp.

some oxidizable constituents such as xylans in wood pulps which are more resistant to ozone than cellulose itself. This can be seen from Table 1 where composition of wood sugars before and after ozonization is shown. The hemicellulose (xylan) containing paper pulp has, in fact, consumed about 30% more ozone than the observed value, based on actual glucan in the sample. The net effect is the loss of about 3.5% glucan after oxidation. The increase in the xylan content after oxidation is an artifact of calculation and should be disregarded. The data, however, show that xylans are more resistant to ozone oxidation than glucans (cellulose). This observation is in line with the observations lately made by Parthasarathy et al. (19) regarding the ozonolysis of xylose vs. mannose. They found that xylose was passive under unsaturated ozonolysis conditions, whereas mannoses were active under any condition of ozonolysis. They proposed an ozone initiated anomeric interconversion from α(C1) to β(C1) and vice versa to explain the activity.

The plot of DP_N vs. $[O_3]$ for these pulps (Fig. 3) shows that the chemical pulp depolymerized at a faster rate than either cotton linters or paper pulp. Paper pulps also did not reach the lower DP_N values as those of chemical or cotton linters pulp. The fast depolymerization rate must be linked to accessibility of the wood pulps compared to cotton. The alkaline treatments which wood pulps undergo during delignification opens up the structure. Within limits of experimental accuracy, the X-ray crystallinity of wood pulps was found to be lower than that of cotton linters or α-cellulose.

The rate at which the chains are scissioned and the number of scissions are both related to accessibility and the initial DP of the sample. Initially all pulps show fast chain breaks which eventually slow down at the level off DP (LODP) region. Figure 4 shows that the high DP cotton samples go through many more scissions and thereby consume more ozone till LODP is reached. An interesting correlationship between LODP and rate of chain scissions is shown in Fig. 5 where the extrapolated DP value of the three pulp samples is between 60-100. This LODP value is much lower than the reported value for hydrocelluloses (≅ 200). The reason for this low LODP value seen in the ozone-cellulose reactions is due to two consecutive attacks on cellulose, one by ozone itself and other due to β-alkoxyl elimination reaction observed during viscosity measurements.

In conclusion, the reaction of ozone with celluloses of different origins is dependent on:

1. the cellulose morphology and the cellulose constituents, such as xylans, mannans, etc., plays an important role in the rates with which cellulose is oxidized by ozone.

2. the cellulose pretreatment which may make cellulose more accessible increase the rate of cellulose depolymerization.

3. Although the rate of chain scission depends upon accessibility, however total number of scissions are dependent upon the initial DP.

4. Very low LODP values of 60-100 DP are seen during cellulose-ozone reactions are due to the consequative attack of ozone, followed by alkaline attack by cupriethylenediamine (CED) used during TAPPI-T230 viscosity determinations.

2) Viscosity Behavior of Ozone Oxidized Celluloses

The scheme shown in Fig. 6 was adopted to investigate the action of ozone on viscosity loss of cellulose during ozonization, viscosity loss during viscosity